URSI AP-RASC 2019, New Delhi, India, 09 - 15 March 2019

Multi-instrumental analyses of the September 2017 space weather storm over Brazil

Juliana G. Damaceno*[(1), (2)], Claudio Cesaroni [(1)], Luca Spogli[(1), (3)], Giorgiana De Franceschi[(1)] and Massimo Cafaro[(2)].
(1) Istituto Nazionale di Geofisica e Vulcanologia (INGV), Via di Vigna Murata 605, 00143 Rome, Italy.
(2) University of Salento (UNISALENTO), Via per Monteroni, 73100 Lecce, Italy.
(3) SpacEarth Technology (SET), Via di Vigna Murata 605, 00143 Rome, Italy.

Abstract

Brazil is a region of the Earth daily affected by strong ionospheric variability that may exacerbate during space weather events. In this paper, the ionospheric response to the solar storms that occurred in the first half of September 2017 is analyzed in terms of scintillation and TEC data from ground-based GNSS, ionospheric parameters from ionosondes and in-situ electron density data provided by the ESA Swarm mission. The result shows the complexity of the equatorial ionospheric dynamics under severe geospatial perturbations highlighting the occurrence of a super fountain event during daytime as the effect of a severe geomagnetic storm.

1. Introduction

In early September 2017, several solar events, including flares and a coronal mass ejection (CME), resulted into one of the most severe geomagnetic storm of the current solar cycle [1]. In the specific, an X2.2 flare at 9:10 UT September 6 preluded the X9.3 class solar flare at 12:02 UT, producing a R3-Strong radio blackout [2]. The impact of the coronal mass ejection (CME) caused a G4 level (severe) geomagnetic storm between September 7 and 8 (22:29 UT). In correspondence with the CME arrival, the Kp and Dst geomagnetic indexes reached up to 8 and -142 nT, respectively [3], [4]. The second strongest flare classified as X8.2 happened on September 10 at 15:35 UT, together to a proton particles event by 18:43 UT. The associated CME was mostly directed away from Earth, that was reached on September 12 and 13 with Kp = 5, producing a minor geomagnetic storm (G1) [5]. In the Brazilian region the ionospheric variability exacerbates during space weather events as it encompasses the crests of the Equatorial Ionospheric Anomaly (EIA) [6]. Here ground based and in situ data are used to show the ionospheric plasma dynamics under the September 2017 events, contributing to assess the worst-case scenario for disruption of real time high accuracy GNSS based applications [7].

2. Data

The data include the electron density n_e measured in situ by Swarm satellites Alfa (A) and Charlie (C), flying side by side at a height of 462 km and with 1.5° of longitudinal separation, and satellite Bravo (B), at an altitude of 510 km on an orbit constantly drifting with respect to the other two satellites [8]. The 2 Hz n_e measurements are provided by the Langmuir probe on-board of the Swarm satellites collecting 10 minutes of data in each passage (both dayside and night side passages). In addition, calibrated TEC (1 min) from 143 geodetic dual frequency GNSS receivers of IBGE network is used to estimate spatial variations of TEC [9]. Amplitude scintillation (S_4) index (1 min) is also used from the CALIBRA network (50 Hz receivers) [10] to identify ionospheric irregularities. Finally, data from five digisondes operating in Brazil within the Global Ionospheric Radio Observatory (GIRO) are used probing the bottom-side ionosphere up to the peak of ionospheric plasma density (Figure 1).

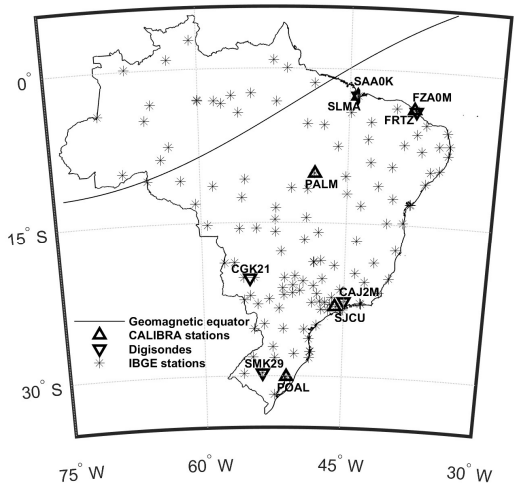

Figure 1. Location of IBGE network, CALIBRA network and digisondes in Brazil used in this study.

3. TEC and Ionospheric Scintillation

The slant TEC (STEC) along the oblique propagation path from IBGE is used to estimate the vertical TEC (VTEC) at the ionospheric pierce point (IPP) [11]. The verticalization allows the data geometry independence [12] and is obtained by applying an appropriate ionosphere mapping function [13]:

$$VTEC = STEC/F(\alpha_{elev}) \quad (1)$$

Where F(α_{elev}) is the obliquity factor, defined as:

$$(\alpha_{elev}) = \frac{1}{\sqrt{1-(\frac{R_e cos\alpha_{elev}}{R_e+H_{IPP}})^2}} \quad (2)$$

α_{elev} is the elevation angle of the satellite, R_e is the Earth radius and H_{IPP} is the height of the ionospheric pierce point, here assumed at 350 km. Scintillations are the effects of the small scale ionospheric irregularities caused by plasma bubbles (PB) on GNSS signals that tend to occur daily in the Brazilian region under the crests of the EIA, during the post-sunset (19 to 01 LT) [12], [14], [15]. The Amplitude Scintillation S_4 is the standard deviation of the received signal power normalized to the average signal power, and it is dimensionless [16]. The vertical S_4 is given by:

$$S_{4\ vertical} = S_{4\ slant} / (F(\alpha_{elev}))^{p+1/4} \quad (3)$$

Where p is a dimensionless variable, which represents the power spectral density of intensity [17].

4. Discussion

The reaction of the equatorial ionosphere over Brazil during the strong solar storm is depicted in Figure 2 in terms of n_e by Swarm satellites A-B-C. The selected tracks cover from the central to the east part of Brazil and are the closest ones to the ground-based network used. During early September, the Swarm A and C satellites crossed this region during nighttime (~22 LT, blue line) and daytime (~10 LT, red line). Swarm B satellite passes at ~03 LT (blue line) and at ~15 LT (red line). Panels a), b) and c) show n_e measured by Swarm A, C and B on September 6 as an example of a quiet condition scenario. The nighttime passages in the disturbed days (8 and 13 September), reveal the presence of n_e irregularities (Figure 2 panels d, e, g, h, blue lines). The nighttime tracks (only A and C satellites, B passage was at different time of the day the September 8 and missing the September 13) show clear signatures of ionospheric plasma depletions (i.e. PB), possibly disturbing the propagation of the GNSS signals. Moreover, in daytime, all of the Swarm satellites reveal an increased n_e, reaching 8.10^5 electrons/cm^3, on September 8. These effects, particularly during the September 8, are probably due to the prompt penetrating electric field in the ionosphere during the day from auroral and sub-auroral latitudes [18]. This affects the plasma uplift (ExB), bringing denser plasma up to Swarm B altitude as shown for 8 September (Figure 2, panel f).

During the post-sunset the Rayleigh-Taylor instability occurs, leading to electron density depletions well captured by satellites A and C (Figure 2, panel g and h).

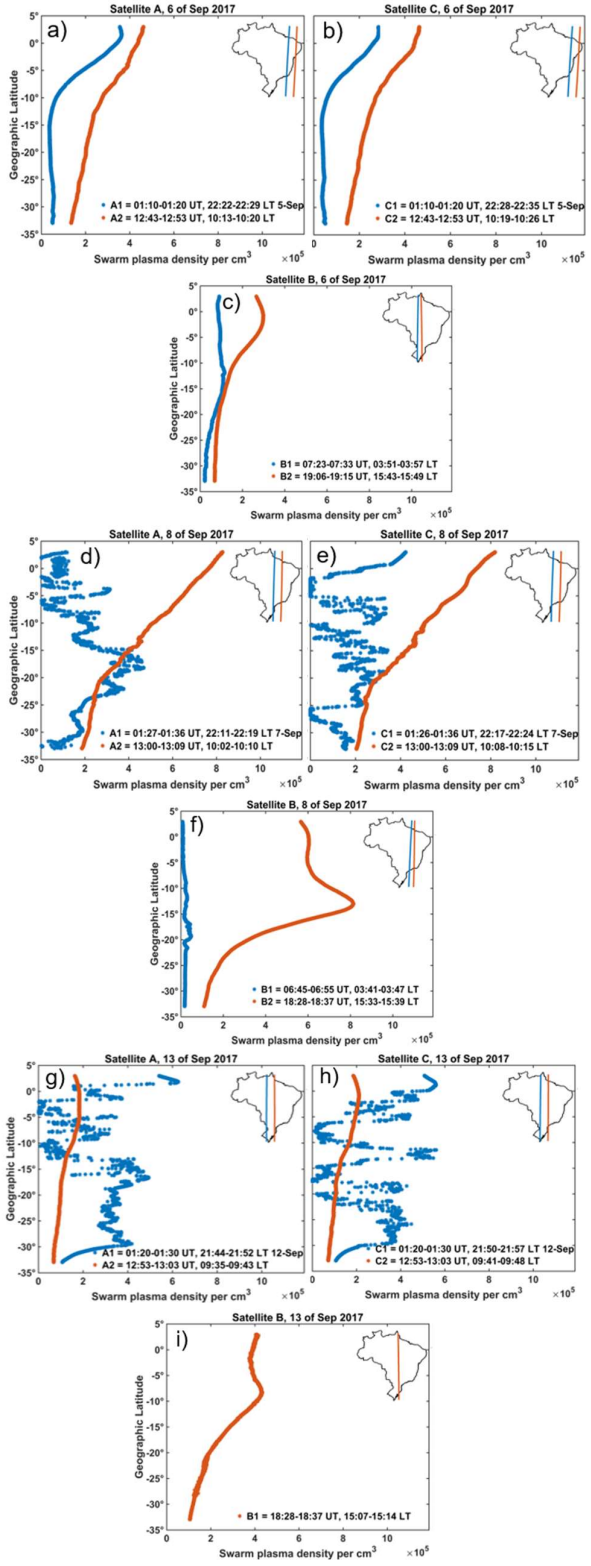

Figure 2. Plasma density profile of satellites A, B and C of Swarm for Brazil region in the days 6, 8 and 13 of September 2017.

Figure 3 reports September 6-14 distribution of TEC retrieved by IBGE as a function of geographic latitude and time. The S_4 by the CALIBRA network (50 Hz receivers) is showed with magenta crosses for $S_4 > 0.3$. The black line superposed indicates the Dst in nT, highlighting the presence of two storms, the second one starting the September 8 [19]. In September 8 the TEC increases and forms two picks of ionization, the first one during daytime indicating that the EIA southern crest intensifies as a result of the CME and expands towards higher latitudes probably due to a super fountain effect [20]. S_4>0.3 appears at TEC gradients expanding to higher latitudes especially during the recovery phase of the storm developed from September 8.

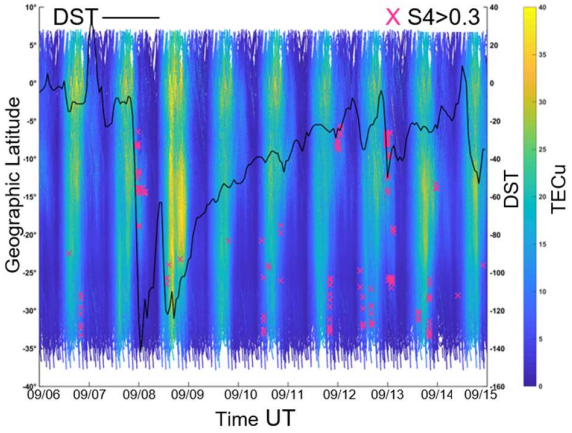

Figure 3. Vertical TEC from IBGE stations for the period 6 - 14 September 2017 along with S_4 scintillation data > 0.3 (magenta crosses) from CALIBRA stations data and the DST index curve (black line).

The digisonde ionograms and the electron density profiles by the Automatic Real-Time Ionogram Scaler with True height software (ARTIST) [21] are presented in Figure 4. The ionograms were recorded at 00:00:00 UT (-3h for approximate LT) of September 8 2017. The two northeast stations (SAA0K and FZA0M) show the presence of strong range spread-F, a signature of PB irregularities that make the vertical electron density profile unreliable. CGK21 station also present some traces of alteration by Rayleigh-Taylor instability. The other stations, SMK29 and CAJ2M show typical mid-latitude night-time ionograms with very well defined traces of the F layer.

5. Conclusions

A deeper understanding of the roles played by different geospatial storm indicators on the equatorial plasma dynamics can contribute to the improvement of models feeding mitigation techniques against the effects of the ionosphere on GNSS based techniques. The multi-instrument data analysis performed over Brazil referred to the September 2017 space weather events shows the high variability of the ionospheric plasma as function of the height, time of the day and latitudes.

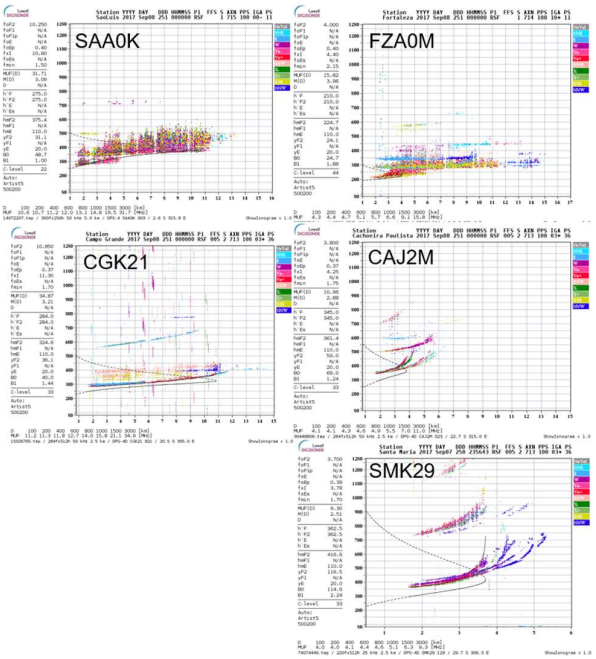

Figure 4. Digisondes operating in Brazil from the Global Ionospheric Radio Observatory (GIRO): a) Sao Luis (SAA0K), b) Fortaleza (FZA0M), c) Campo Grande (CGK21), d) Santa Maria (SMK29) and e) Cachoeira Paulista (CAJ2M).

The nighttime passage of the Swarm satellites over Brazil indicates the formation of plasma bubbles the 8 and 13 September 2017, clearly identify until an altitude of 460 km (Swarm satellites A and C) at least the September 8, as Swarm B data are missing the 13 September. The September 8 during daytime, the plasma density intensify and moved to high altitudes (510 Km) as showed by satellite B, especially in the region of the southern EIA crest. The CME induces two maxima of TEC elongated towards higher latitudes. Scintillation occurrence (for S_4>0.3) tends to increase still towards higher latitudes during the recovery phase of the storm. Digisondes confirm the nighttime occurrence of PB irregularities during nighttime of September 8, the signatures (strong range spread F) decreasing with increasing the latitude.

6. Acknowledgements

The authors wishes to express sincere thanks to the TREASURE project, funded by the European Union's Horizon 2020 research and innovation programme under the Marie Skłodowska-Curie Actions grant agreement No 722023 http://treasure-gnss.eu. Thanks to data providers: Analysis Center for Geomagnetism and Space Magnetism Faculty of Science, Kyoto at http://wdc.kugi.kyoto-u.ac.jp; GIRO data (http://spase.info/SMWG/Observatory/GIRO); European Space Agency (ESA) for the Swarm data (https://earth.esa.int/web/guest/swarm/data-access); CIGALA/CALIBRA Network for ISMR data (http://is-cigala-calibra.fct.unesp.br); IBGE for GPS data over Brazil

(http://www.ibge.gov.br/home/geociencias/geodesia/rbmc/rbmc_est.php).

7. References

1. Chertok IM, Belov A V, Abunin AA. Solar Eruptions, Forbush Decreases and Geomagnetic Disturbances from Outstanding Active Region 12673. Sp Weather. 2017. doi:10.1029/2018SW001899.

2. Yasyukevich Y, Astafyeva E, Padokhin A, Ivanova V, Syrovatskii S, Podlesnyi A. The 6 September 2017 X-class solar flares and their impacts on the ionosphere , GNSS and HF radio wave propagation. 2017;(September):1-15. doi:10.1029/2018SW001932.

3. Augusto CRA, Navia CE, de Oliveira MN, et al. Relativistic proton levels from region AR2673 (GLE \#72) and the heliospheric current sheet as a Sun-Earth magnetic connection.2018;2673:1-9. ttp://arxiv.org/abs/1805.02678.

4. Kirilov Y, Bulgarian T, Ohridski K. Analysis of extreme solar activity in early september 2017 : G4 – severe geomagnetic. Comptes rendus l'Académie Bulg des Sci Sci mathématiques Nat. 2017;72(September).

5. Wang H, Yurchyshyn V, Liu C, Ahn K, Toriumi S, Cao W. Strong Transverse Photosphere Magnetic Fields and Twist in Light Bridge Dividing Delta Sunspot of Active Region 12673. Res Notes AAS. 2018;2(1):8. doi:10.3847/2515-5172/aaa670.

6. Venkatesh, K., et al. "Electrodynamic disturbances in the Brazilian equatorial and low ‐ latitude ionosphere on St. Patrick's day storm of 17 march 2015." J. Geophys Res Sp Phys 2017 122.4: 4553-4570. doi.org/10.1002/2017JA024009

7. Park J, Sreeja V, Aquino M, et al. Performance of ionospheric maps in support of long baseline GNSS kinematic positioning at low latitudes. Radio Sci. 2016;51(5):429-442. doi:10.1002/2015RS005933.

8. Lu H, Knudsen D, Haagmans R. Swarm – An Earth Observation Mission investigating Geospace. 2008;41:210-216. doi:10.1016/j.asr.2006.10.008.

9. Ciraolo L, Azpilicueta F, Brunini C, Meza A, Radicella SM. Calibration errors on experimental slant total electron content (TEC) determined with GPS. J Geod. 2007;81(2):111-120. doi:10.1007/s00190-006-0093-1.

10. Vani BC, Shimabukuro MH, Galera Monico JF. Visual exploration and analysis of ionospheric scintillation monitoring data: The ISMR Query Tool. Comput Geosci. 2017;104:125-134. doi:10.1016/j.cageo.2016.08.022.

11. Mannucci AJ, Wilson BD, Yuan DN, Ho CH, Lindqwister UJ, Runge TF. A global mapping technique for GPS-derived ionospheric total electron content measurements. Radio Sci. 1998;33(3):565-582. doi:10.1029/97RS02707.

12. Spogli L, Alfonsi L, Romano V, et al. Assessing the GNSS scintillation climate over Brazil under increasing solar activity. J Atmos Solar-Terrestrial Phys. 2013;105-106:199-206. doi:10.1016/j.jastp.2013.10.003.

13. Cesaroni, C., Spogli, L., Alfonsi, L., De Franceschi, G., …& Bougard, B. L-band scintillations and calibrated total electron content gradients over Brazil during the last solar maximum. J. Space Weather Space Clim. 2015, 5, A36. doi.org/10.1051/swsc/2015038

14. Aarons J. The role of the ring current in the generation or inhibition of equatorial F layer irregularities during magnetic storms. Radio Sci. 1991;26(4):1131-1149. doi:10.1029/91RS00473.

15. Marques HA, Marques HAS, Aquino M, Veettil SV, Monico JFG. 2018. Accuracy assessment of Precise Point Positioning with multi-constellation GNSS data under ionospheric scintillation effects. J. Space Weather Space Clim. 8: A15. doi:10.1051/swsc/2017043.

16. Briggs BH, Parkin IA. On the variation of radio star and satellite scintillations with zenith angle. J Atmos Terr Phys. 1963;25(6):339-366. doi:10.1016/0021-9169(63)90150-8.

17. Wernik AW, Alfonsi L, Materassi M. Scintillation modeling using in situ data. Radio Sci. 2007;42(1):1-21. doi:10.1029/2006RS003512.

18. Tsurutani B, Mannucci A, Iijima B, et al. Global dayside ionospheric uplift and enhancement associated with interplanetary electric fields. J Geophys Res Sp Phys. 2004;109(A8):1-16. doi:10.1029/2003JA010342.

19. Li G, Ning B, Wang C, et al. Storm-Enhanced Development of Postsunset Equatorial Plasma Bubbles Around the Meridian 120°E/60°W on 7-8 September 2017. J Geophys Res Sp Phys. September 2018:1-14. doi:10.1029/2018JA025871.

20. Mannucci AJ, Tsurutani BT, Iijima BA, et al. Dayside global ionospheric response to the major interplanetary events of October 29-30, 2003 "Halloween Storms." Geophys Res Lett. 2005;32(12):1-4. doi:10.1029/2004GL021467.

21. Reinisch BW, Huang X, Galkin IA, Paznukhov V, Kozlov A. Recent advances in real-time analysis of ionograms and ionospheric drift measurements with digisondes. J Atmos Solar-Terrestrial Phys. 2005;67(12 SPEC. ISS.):1054-1062. doi:10.1016/j.jastp.2005.01.009.